Real-Time Forecasting and Reanalysis During AOSN-II Using the Harvard Ocean Predicition System

Abstract

During the August-September 2003 AOSN-II experiment, the Harvard Ocean Prediction System (HOPS) and Error Subspace Statistical Estimation (ESSE) system were utilized in real-time to forecast physical fields and uncertainties, assimilate various data (CTD, AUVs, gliders, SST), provide suggestions for adaptive sampling, and guide dynamical investigations. 22 sets of real-time nowcasts and forecasts were issued, including 10 sets of real-time ESSE error forecasts. Adaptive sampling recommendations were suggested on a routine basis. The forecasts, data analyses and daily dynamical descriptions were distributed via a local web site. Results from the operational forecasts are presented as well as forecast skill estimates. Following the real-time experiment, a reanalysis led to improved procedures and parameters, resulting in a continuous dynamical simulation of the experimental period. Finally, multi-model techniques were used to further improve the simulation skill by combining HOPS and ROMS simulations.

Introduction

Start with an AOSN-II context.

- *Make sure to describing the sampling, especially the 3 synoptic coverage Pt Sur CTD surveys.*
- *Historically expect sustained upwelling events (NW wind) separated by relaxation events.*

Follow with a generic description of HOPS/ESSE

- *Move some of the description of 2-way nesting that's currently in the results section here.*

Real-Time Methodology

The real-time methodology was chosen to be able to provide daily forecast products in a timely manner. The constraints defining "timeliness" were: (1) the process would start each morning so as to include the most recent data and atmospheric forcings and (2) the forecasts need to be finished, examined and have their products generated by the late afternoon briefing. The canonical day's operations proceeded as follows. First, the most recent data and atmospheric forcings were gathered and processed for use in the HOPS PE model. An initialization was generated from the previous day's simulation, from the fields corresponding to 0000Z on the previous day. Several PE simulations would then be run, using the updated atmospheric forcings and assimilating the new data but with different model parameters. The best simulation would be chosen and the forecast products generated and disseminated.

Domains

Four domains were designed to produce two sets of telescoping 2–way nested simulations. The innermost domain, designated the "Data Domain", was designed to contain the region of primary sampling around Monterey Bay. The Data Domain contained the

upwelling centers at Point Ano Nuevo and Point Sur. The middle domain, designated the "Off Shore Domain", was designed to provide a buffer for the Data Domain while capturing the longest expected plumes. The Off Shore Domain extended over 300km offshore, to the edge of the California Current Region and was roughly centered in the north/south directions around Monterey Bay. Finally, two different choices were designed for the largest domain, designated the "California Current Domains". These domains both extended offshore enough to cover the region of the California Current, differing in their north/south extents.

- *Extents of California Current and California Under Current?*
- *Domains parameters?*
  - *vertical discretization?*
  - *topographic conditioning?*
- *Expected Run times*
- *Any reason to keep "California Current Domains"?*
- *Reference the domain selection page?*

For the real-time experiment the California Current Domains were abandoned and the Off Shore Domain was only used as boundary control for the Data Domain. In fact the Data Domain was run both 2-way nested to the Off Shore Domain and in "stand alone" mode with open boundary conditions.

Oceanographic Data Processing

On a daily basis, the available CTD profiles and WHOI and SIO glider pseudo-profiles were collected and converted to the HOPS ASCII format. The data were first visually inspected on an instrument by instrument basis to ensure internal consistency. In some cases, a median filter was applied to de-spike noisy data. After this first pass of quality control, the profiles from different instruments were visually compared to each other and to the most recent Pt. Sur CTD survey. The outliers were identified and removed, retaining as much data as possible (e.g. If a profile fell within the common envelope in its surface and deep values but was far off in the thermocline, the thermocline portion would be removed and the remainder broken into 2 profiles, one shallow and one deep.).

Intermittently, NPS would fly an aircraft SST mission. When this data was available, it was gathered and binned. The binning consisted of splitting the time "coordinate" of the SST data into 100 second bins and averaging the data in each bin, producing a nominal 5km along-track resolution. These surface values were extended in the vertical by assuming a mean mixed-layer depth of 5m and copying the surface temperature value to 5m.

Double check the nominal along-track resolution.

The *in situ* and SST profiles were gathered processed through the HOPS objective analysis package. Prior to this collection, the glider data were thinned by *(how much?)*. This was done to speed the objective analysis. The data were then analyzed with the correlation parameters in table 1, depending on whether the analyzed fields were to be used to initialize a simulation or to be assimilated into a simulation. The output of the objective analysis are three dimensional fields of temperature, salinity, dynamic height and their associated errors. These fields are located on the same horizontal grid as the PE domain, but are on flat levels in the vertical. The temperature and salinity are interpolated

to the PE terrain-following vertical coordinates. The dynamic height is first differentiated to produce horizontal velocities on the flat levels. These velocities are then interpolated to the terrain-following coordinates, and decomposed into a depth averaged component and an "internal" (remainder) component. The depth averaged component is used to generate a transport streamfunction, to ensure the non-divergence of transport.

Atmospheric Forcing

COAMPS analysis and 72 hour forecast fields, received from `ftp.nrlmry.navy.mil` on a twice daily basis, were used to generate atmospheric forcings for the AOSN-II HOPS simulations. The COAMPS fields were available on four different resolution lambert conformal projection COAMPS grids. The nominal 0.03° resolution fields were used to generate forcings for the Data Domain. The nominal 0.1° fields were used to generate forcings for the Offshore domain.

The wind stress fields from COAMPS were bi-cubically interpolated to the HOPS grids, rescaled from (N/m^2) to ($dyne/cm^2$) and decomposed in terms of the direction vectors aligned with the HOPS grids. Special care was taken to resolve the mismatch of HOPS and COAMPS land masks. COAMPS wind stress values are, on average, an order of magnitude higher over the land than over the sea. Hence, discrepancies in the land masks could lead to excessive values of the wind stress on the HOPS grids near the coasts. To control this problem, wind stress values from COAMPS sea-points were extrapolated to COAMPS land-points prior to interpolation.

The surface net heat flux into the ocean (W/m^2) was composed as the sum of the shortwave radiation, the longwave radiation, the sensible heat flux and the latent heat flux; all of which were directly available from the COAMPS output. The resultant net heat flux was then bi-cubically interpolated to the HOPS grids. Similarly, the shortwave radiation was also bi-cubically interpolated to the HOPS grids, for use in biological simulations.

The net surface water flux out of the ocean (cm/day) was calculated as the difference of evaporation minus precipitation. Evaporation was calculated as the latent heat flux divided by the latent heat of evaporation. The latent heat of evaporation was computed from the formula $2.5008(10^6) - 2.3(10^3)T_{air}$, where T_{air} was the air temperature obtained from COAMPS. The resulting evaporation was then converted from ($kg/(m^2s)$) to (cm/day). The total precipitation was obtained directly from COAMPS, merely needing a conversion from (mm in 12 hours) to (cm/day). The net water flux was bi-cubically interpolated to the HOPS grids.

What quality control was applied?

- *Do the pre-experiment (ICON, Rosenfeld) tests need to be mentioned? Where?*

Adaptive Sampling

Need something here.

Product Dissemination

There were 2 paths for the dissemination of HOPS products. The first was the web page `http://people.deas.harvard.edu/ leslie/AOSNII/`. This page provides links to plots of the HOPS real-time nowcast/forecast fields. The horizontal plots were provided at 4 depths, pre-selected based on the vertical structure of the data: surface, 10m (base of

mixed layer), 30m (middle of thermocline), and 200m (California Under Current region). Vertical sections were made coming out of points Ano Nuevo and Sur and out of the center of Monterey Bay. Additional links include special products, pre-experiment planning documents and post-experiment on-going analyses.

The second path was the MBARI server. NetCDF output files from the issued HOPS PE forecasts were uploaded to the server. In addition, some specially formatted output for the LCS analysis were also uploaded.

Real-Time Results

Data

Need a comparison of AOSN-II to history/climatology.

Figure 1 shows the measured winds at the M1 and M2 moorings. In the period of August 8-17, both moorings show a sustained upwelling event, with a brief weakening around August 15. Between August 17-21, there is a slight disagreement between the two, with M2 showing a continuation of the upwelling event and M1 showing both weakening and less uniformity in direction. Both show a relaxation event between August 21-24. Again, between August 24-27, there is a disagreement between the two, with M2 showing the beginning of the upwelling event and M1 showing less uniformity in direction. Between August 27 and September 1, the winds are generally in an upwelling favorable direction, although the strength is falling off after August 29. Both show a relaxation event between September 2-5.

Real-Time Modeling

The real-time modeling effort can be divided into three periods, according to the Pt Sur surveys. Prior to August 7, the first Pt Sur survey data were not yet completed and processed. The forecasts issued in those times were initialized with July 2003 data combined with historical synoptic surveys. In the period August 7-26, the processed first survey was available but not the second. The forecasts were either directly initialized with the first survey or were restarts from forecasts that, ultimately, traced back to initializations from the first survey. After August 26, the second survey was processed and the forecasts were either initialized from the second survey or from restarts that traced back to the second survey.

The HOPS PE model was run in three different configurations. The first was the "Stand alone Data Domain". In this case the PE model was configured to run in the Data Domain with open boundary conditions applied to the external boundaries. Any data assimilation would be done using the Optimal Interpolation (OI) method. This configuration was always the first one tried in a new situation. It's simplicity facilitated a rapid search for a stable regime. The second was a 2-way nested configuration (Sloan 1996) with one model set up for the Data Domain and another for the Off Shore Domain. Interprocess communication updates the Off Shore Domain with information from the Data Domain in the region of overlap and updates the boundaries of the Data Domain with information from the updated Off Shore Domain. Traditionally, this provides a superior representation of the lateral forcing on the smaller domain while simultaneously reducing boundary noise. In this instance, there was no significant data outside of the Data Domain, hence no

reliable estimate of the lateral forcing. The nesting did provide improved stability by reducing boundary noise. The lack of *in situ* data outside of the Data Domain, coupled with the atypical conditions, introduced some difficulty in initializing the Off Shore Domain. *Some archaeology is needed to be sure exactly what was done. It looks like a shifted GDEM was used.* The third configuration was the "ESSE" configuration. This was essentially the "Stand alone Data Domain" with assimilation being done via the ESSE methodology not OI. This configuration had the superior data assimilation methodology which also produced estimates of the forecast error.

All simulations were made with a 300 second time step. The lateral open boundary forcing was parameterized with the implicit Orlanski radiation condition (Orlanski, 1976) for the tracer, velocity and transport streamfunction variables. For the rate of change of barotropic vorticity, the boundary condition used was most often a Courant-Freidrichs-von Neumann radiation condition derived by Spall and Robinson (1989), although in the last third of the experiment, the Orlanski condition was used. The horizontal sub-gridscale was parameterized by a Shapiro filter (Shapiro, 1970). In particular a fourth order filter was used for tracers and momentum, a (stronger) second order filter was used for the rate of change of barotropic vorticity. In the vertical, the sub-gridscale was parameterized by a second order diffusion term where the coefficients are function of the Richardson number, following the Pacanowski and Philander (1981) scheme. The peak viscosity/diffusivity was set to 50 cm^2/s, the background viscosity was set in the range 0.1-0.2 cm^2/s, and the background diffusivity was set in the range 0.01-0.02 cm^2/s. Near the surface, the vertical viscosity and diffusivity coefficients are bounded below by values (30 cm^2/s for viscosity and 5-6 cm^2/s for diffusivity) to reflect wind mixing. The depth to which these mixing bounds are applied was proportional to $(\|\tau\|/\rho_0)^{\frac{1}{2}}/f$ where τ is the wind stress, ρ_0 is the mean density of seawater and f is the coriolis factor. The nondimensional constant of proportionality was set in the range 0.15-0.22. This wind mixing depth was never allowed to be shallower than 1m or exceed 40m. At depths where the water column is gravitationally unstable, the vertical viscosity/diffusivity were bounded below by 50 cm^2/s. Finally, a Rayleigh friction parameterization of drag induced by the bottom or coasts (Lermusiaux 1997) was used. In both cases, the temporal decay scale was 3600s and the spatial decay was 1.5 (model levels from the bottom or grid points from the nearest coast, respectively).

Once each simulation day, data would be assimilated into the model. The nominal assimilation time was 1200Z. Temperature and salinity data within ± 18 hr of that time would be gathered and objectively analyzed with the assimilation scales in table 1. These fields were then processed for the PE model terrain-following coordinates and to generate a geostrophic internal mode velocity. These temperature, salinity and internal velocity fields were then assimilated into the model, according to their associated error fields. Rather than "shocking" the system by simply inserting the assimilation fields at the desired times, the fields are first assimilated earlier with down-weighted assimilation weights ("ramping in"). The schedule used, along with the down-weighting weights, are presented in table 2. One of the first things to notice is that the weights for assimilating the internal mode geostrophic velocity are smaller than those for temperature and salinity, reflecting a desire to avoid completely overwriting the PE physics with geostrophy. The second thing is that a "ramp out" cycle, weak post-assimilation time assimilation, is included. Note that prior

to the August 19 issued forecast, the "ramp out" cycle was not used. Further, on August 19-21, and 28-30, forecasts where the weights for assimilating internal mode velocity were further decreased by a factor of 2 were selected for issuance. *ESSE points?*

In the period 4 August - 3 September 2003, forecasts were issued on 23 days, as indicated in table 3. Starting with the 30m fields, the forecasts show a general cyclonic circulation in Monterey Bay. They have, in general, a southward flow along the shelf which flows across the mouth of Monterey Bay. Offshore, an inflow in the western boundary bends north providing a general northward flow. Inshore of this flow, but off the shelf, an anticyclonic eddy is usually present. The exact size, shape and position of this eddy are fairly variable. The situation at the surface is very similar except during the periods of strong upwelling favorable winds. In these periods, the winds dominate resulting in broad generally southward flow across the domain. The surface also shows a band of warmer water lining the coast of Monterey Bay, occasionally protruding out the northern edge of the mouth of the bay. At 200m, there is a general northward flow originating from the western boundary, sometimes accompanied by a northward flow along the slope. The eddy opposite Monterey Bay is still visible at this depth, sometimes even more so than at shallower depths. *More work needed on wind response. Muddled by differing methodologies.* Figure 3 shows the issued surface fields at the central times of the earlier identified upwelling/relaxation periods and in the transition periods between.

The issued forecasts also highlight some of the differences in the different PE configurations. On August 12 and 13, multiple forecasts were issued to illustrate some of the uncertainty in the forecasts. An important difference can be seen at 200m (figure 4). Although a three cases show general northward flow, the stand-alone cast has 2 distinct branches. The first enters from the western boundary and turns north. The second enters from the southern boundary by Point Sur and flows north along the slope. This second branch pushes an eddy, originally opposite Monterey Bay, northward along the slope until, by the August 13, it is opposite point Ano Nuevo. By contrast, the nested configuration has a large, anticyclonic half eddy on the southern boundary. This boundary eddy appears to choke off the along slope branch of the northward flow. As a result, the eddy that was originally opposite Monterey Bay does not advect nearly so far north by August 13. The inflow from the western boundary is broader and further south. It still bends north in a broad northward flow that fills most of the domain. The ESSE forecast is more similar to the stand-alone case, in that it has 2 branches. The inflow from the west is much broader, covering the northern 2/3 of the western boundary.

On ten days during the real-time experiment, forecasts of the estimated model error were issued (table 3). These error forecasts provided useful guidance for the adaptive sampling recommendations.

- *Details on the one recommendation actually carried out*
- *Was the ESSE optimized adaptive sampling carried out in real time?*
- *Forecast Skill*
  - *Reference LCS success*
  - *Refer back to upwelling and relaxation features*

To assess the skill in the real-time forecasts, two skill metrics are introduced. The first is the root-mean-square error. Denoting the set of forecast values $\mathbf{T_f}$ and the corre-

sponding set of observed values $\mathbf{T_o}$ then the root-mean-square forecast error, $\mathrm{Trms}_{\mathrm{Forecast}}$, is simply the root mean square of the difference between $\mathbf{T_f}$ and $\mathbf{T_o}$. Similarly the RMS persistence error, $\mathrm{Trms}_{\mathrm{Persistence}}$, is obtained by replacing the forecast values with the initialization values $\mathbf{T_i}$ in the root-mean-square difference. A forecast is said to have skill when the RMS forecast error is less than the RMS persistence error. Figures 5 and 6 show differences between the RMS persistence errors and the RMS forecast errors for the one and two day forecasts of temperature and salinity issued in real-time. The observations are the assimilation fields corresponding the the forecast days, in the regions where the nondimensional observation OA error is less than or equal to 0.25. The RMSEs are computed at 2m(surface), 10m(base mixed layer/ top of thermocline), 30m(middle of thermocline), 150m(California Under Current), 300m(deep) and the average of all the points on those levels. Both temperature and salinity show, on average, skill in the one and two day forecasts. Both show skill near the surface and a lack of skill at depth. This lack of skill at depth is due, in part, to the decreased variability at depth. The decrease in variability means that it is easier for any model error to exceed the actual changes. The temperature shows better skill at one day than at two days. The salinity shows, on average, the same skill at one and two days.

The second skill metric is the Pattern Correlation Coefficient (PCC) or Anomaly Correlation Coefficient. Using the notation for the RMS errors, the forecast PCC for temperature, $\mathrm{Tpcc}_{\mathrm{Forecast}}$, is given by

$$\mathrm{Tpcc}_{\mathrm{Forecast}} = \frac{\left(\mathbf{T_f} - \overline{\mathbf{T_o}}\right)\left(\mathbf{T_o} - \overline{\mathbf{T_o}}\right)^T}{\left\|\mathbf{T_f} - \overline{\mathbf{T_o}}\right\|\left\|\mathbf{T_o} - \overline{\mathbf{T_o}}\right\|} \quad . \tag{1}$$

Note that in equation 1 the large-scale mean, $\overline{\mathbf{T_o}}$, has been introduced. In this work, $\overline{\mathbf{T_o}}$ is a weighted mean of the the observations, with the weighting function $e^{-(r/45)^2}$ where r is the distance (km) between an observation point and the point where the mean is being evaluated. Note also that the scaling in equation 1 is such that $\mathrm{Tpcc}_{\mathrm{Forecast}} \in [-1\ 1]$ with perfect correlation given by $\mathrm{Tpcc}_{\mathrm{Forecast}} = 1$, a complete lack of correlation given by $\mathrm{Tpcc}_{\mathrm{Forecast}} = 0$ and perfect anticorrelation given by $\mathrm{Tpcc}_{\mathrm{Forecast}} = -1$. As in the RMS error, the persistence PCC, $\mathrm{Tpcc}_{\mathrm{Persistence}}$, is obtained by replacing $\mathbf{T_f}$ with $\mathbf{T_i}$ in equation 1. Using PCC, a forecast is said to have skill if $\mathrm{Tpcc}_{\mathrm{Forecast}} > \mathrm{Tpcc}_{\mathrm{Persistence}}$. Figures 7 and 8 show the difference between the forecast and persistence PCC's for the real-time issued one and two day forecasts. As with the RMS errors, both show over-all skill, skill in the upper ocean and a lack of skill at depth. The temperature shows similar skill at the one and two day forecasts. The salinity shows, on average, slightly better skill at two days than at one.

Reanalysis Methodology

The real-time forecasts present a series of realizations of the ocean in and around Monterey Bay. These realizations are, however, somewhat disjoint. This arises from three main sources: (1) different configurations (stand-alone OI, nested-OI and stand-alone ESSE) were employed for different forecasts (table 3 and figure 4), (2) different starting conditions were employed at different times in the experiment (historical data, data during

first Pt Sur cruise and data during second Pt Sur cruise), and (3) model parameters were being tuned during the experiment. These differences prevent the real-time forecasts from being simply concatenated together and used for serious dynamical studies. Therefore a reanalysis of the AOSN-II data and forecasts was performed to provide a single, continuous realization of the experiment.

The first reanalysis series was modest in scope. The goal was to quickly produce a tuned continuous 4D representation of the oceans in the AOSN-II region using the real-time methodology with data and parameter improvements. To speed the process, the simplest configuration (stand-alone Data domain with OI assimilation) was used. To create initialization and boundary data, three objective analyses were made using the "initialization" parameters in table 1. *Some comment on the version of the data used.* The first was an analysis for 00Z on 6 Aug 2003 using Pt Sur CTDs, WHOI & SIO glider and NPS SST data in the period 2-6 Aug 2003. The second was an analysis for 00Z on 23 Aug 2003 using Pt Sur and John Martin CTDs, WHOI & SIO glider and NPS SST data in the period 21-25 Aug 2003. The third was an analysis for 00Z on 5 Sep 2003 using Pt Sur CTDs in the period 3-6 Sep 2003. These analyses were then processed (with a 1250m level of no-motion) to produce an initial condition and time-evolving boundary data. These boundary data were used in the following manner: for temperature and salinity the simulation boundary conditions were simply linear temporal interpolations of the boundary data, with persistence after 5 Sep; for internal mode velocity, the time interpolated boundary data were used as the "control fields" in the boundary condition relaxation scheme (Appendix I). The transport streamfunction and barotropic vorticity used Orlanski radiation conditions.

Thirty-one assimilation fields were created by daily objective analyses of August 6 - September 06 2003 Pt. Sur, John Martin and Pt. Lobos CTDs; WHOI and SIO gliders; and NPS aircraft SST with the correlation scales in table 1 and analysis dates of 7 Aug - 6 Sep, 2003 at 1200Z. For each analysis, only data within $\pm$ 18 hours of the analysis time were used. From the mapped temperature and salinity fields, velocity estimates were obtained by geostrophic integration with an assumed level of no motion of 1250m. The assimilation into the simulation followed the schedule and weights of table 2, with the provisio that the weights for assimilating internal velocity were half those in the table.

Reanalysis Results

The first series of experiments were made to improve long-term stability, primarily by controlling instabilities in the southern boundary by Point Sur. The three most important changes in this regard were: (1) the use of time-varying boundary, described in the previous section; (2) additional smoothing of the topography in the neighborhood of Point Sur, restricting the maximum slope to 0.11; and (3) weakening the relaxation parameters (table 5) used in the boundary condition relaxation scheme. Additionally, to improve coastal currents, the coastal friction was weakened by increasing the relaxation timescale (7200 s). Otherwise, the run parameters were the same as those used at the end of the real-time experiment.

- Skill Metrics
- Upwelling and relaxation

- with pictures
- Uses

Multi-Modeling

Oleg's text here.

Appendix I: New Open Boundary Conditions

The southern open boundary by Point Sur was especially problematic and limiting to simulation duration. To handle this boundary, two variations on the standard Orlanski radiation condition were used. The first was based on relaxing the predicted boundary values to a control field. The second was based on the nesting boundary conditions of Perkins *et al.* (1997).

Boundary condition relaxation

"Boundary condition relaxation" is a relaxation-type forcing applied to the predicted boundary values to try to restrict them from running wild. The basic form of this forcing is[1]

$$u_{b,i,k}^{n+1} = ubc_{b,i,k}^{n+1} - \omega_{b,k}\left(u_{b,i,k}^{n-1} - u_{data_{b,i,k}}\right) \tag{2}$$

where u is the variable whose boundary values are being sought, b is the boundary index, i is the along-boundary index, k is the depth index, ubc is the predicted boundary value, u_{data} is some additional data for u along the boundaries and $\omega_{b,k}$ is the relaxation weight. The relaxation weight is computed from[2]

$$\omega_{b,k} = \frac{2\Delta t}{\tau_{1b} + \tau_{2b}\left[e^{\gamma_b\left(\frac{1-k}{K-1}\right)} - e^{-\gamma_b}\right]} \tag{3}$$

where Δt is the time step (s), τ_1 is the base decay rate (s), τ_2 is the depth decay rate (s), γ is a nondimensional depth decay factor and K is the total number of model levels. For model levels shallower than $K - k_{fix}$, the local velocity $u_{b,i,k}^{n-1}$ is examined and, if found to be outflow[3], the weight $\omega_{b,k}$ is multiplied by $\frac{1}{4}$.

[1] Review code, I seem to be using $u_{b,i-1,k}^{n-1}$ instead of $u_{b,i,k}^{n-1}$.

[2] There may be a computational issue in the evaluation of the first exponential argument. I've coded `float((1-k)/kmm1)` instead of `float(1-k)/float(kmm1)`.

[3] Review code, I seem to be testing $u_{b,i-1,k}^{n}$ instead of $u_{b,i,k}^{n}$.

	Initialization		Assimilation	
	Synoptic	**Mean**	**Synoptic**	**Mean**
Decay (km)	15	45	5	25
Zero-Cross (km)	37.5	112.5	12.5	50
Time-Decay (day)	10	1000	1	80

Table 1: Objective Analysis correlation parameters.

Time	**Weights (T,S)**	**Weights ($\vec{U}_{internal}$)**
t_{assim} **- 0.25**	0.333	0.167
t_{assim} **- 0.125**	0.666	0.333
t_{assim}	0.999	0.5
t_{assim} **+ 0.25**	0.333	0.167

Table 2: Optimal Interpolation assimilation ramping parameters.

	Stand Alone	Nested	ESSE	ESSE Error
Aug 4	X			
Aug 6	X			
Aug 7	X			
Aug 8	X			
Aug 9	X			
Aug 10	X			X
Aug 11		X		X
Aug 12	X	X		X
Aug 13	X	X	X	X
Aug 14		X		
Aug 15		X		
Aug 17		X		
Aug 18		X		
Aug 19		X		
Aug 20		X		
Aug 21		X		
Aug 22			X	X
Aug 24			X	X
Aug 26			X	X
Aug 27				X
Aug 28	X			
Aug 29	X			X
Aug 30		X		
Sep 3			X	X

Table 3: Dates and types of issued forecasts.

Boundary	k_{fix}	τ_1 (days)	τ_2 (days)	γ
w	5	1	4	5
s	5	0.1	1.5	5
n	5	0.1	3.9	6

Table 4: AOSN-BC parameters used in real-time forecasts.

Boundary	k_{fix}	τ_1 (days)	τ_2 (days)	γ
w	5	1	4	5
s	5	1	3.9	5
n	5	1	3.9	6

Table 5: AOSN-BC parameters used in reanalysis.

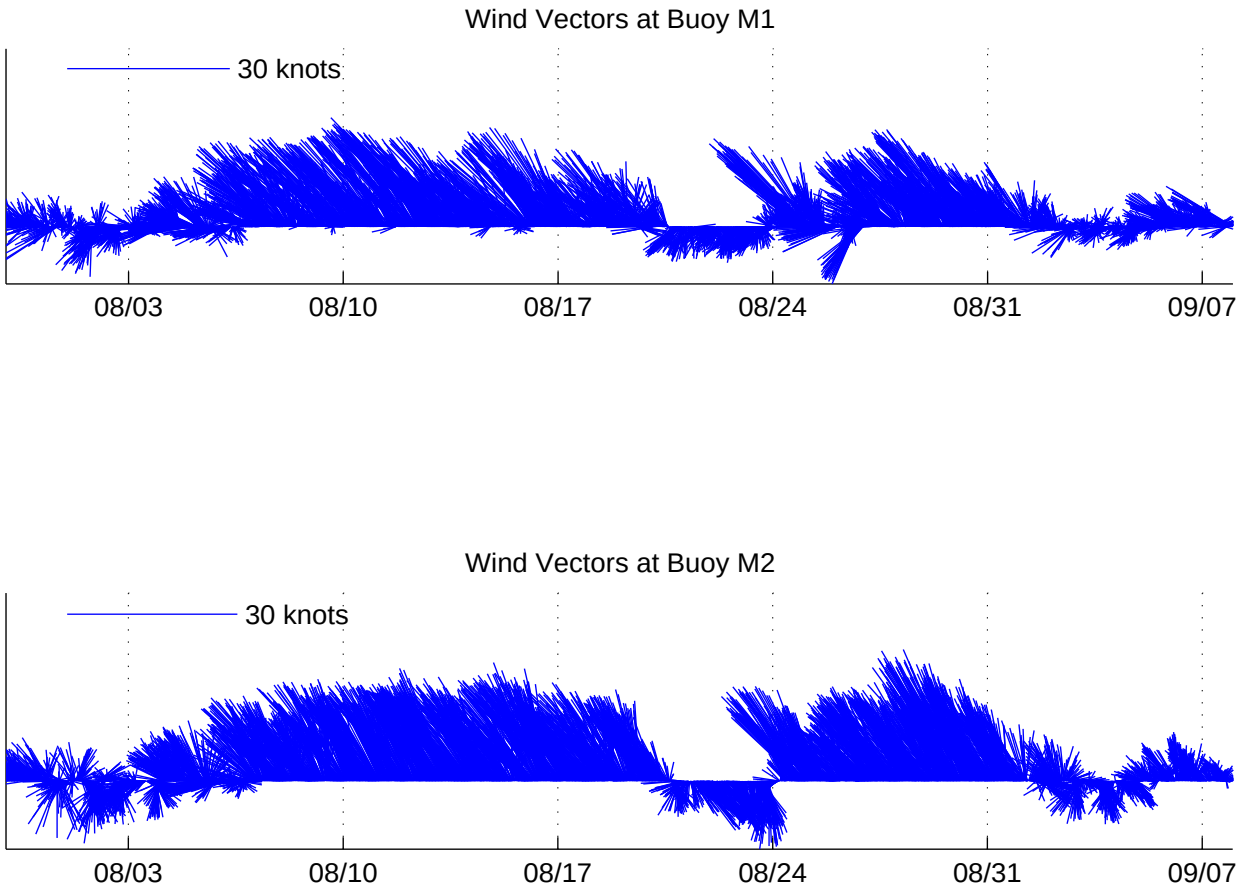

Figure 1 : Wind vectors at the M1 and M2 moorings.

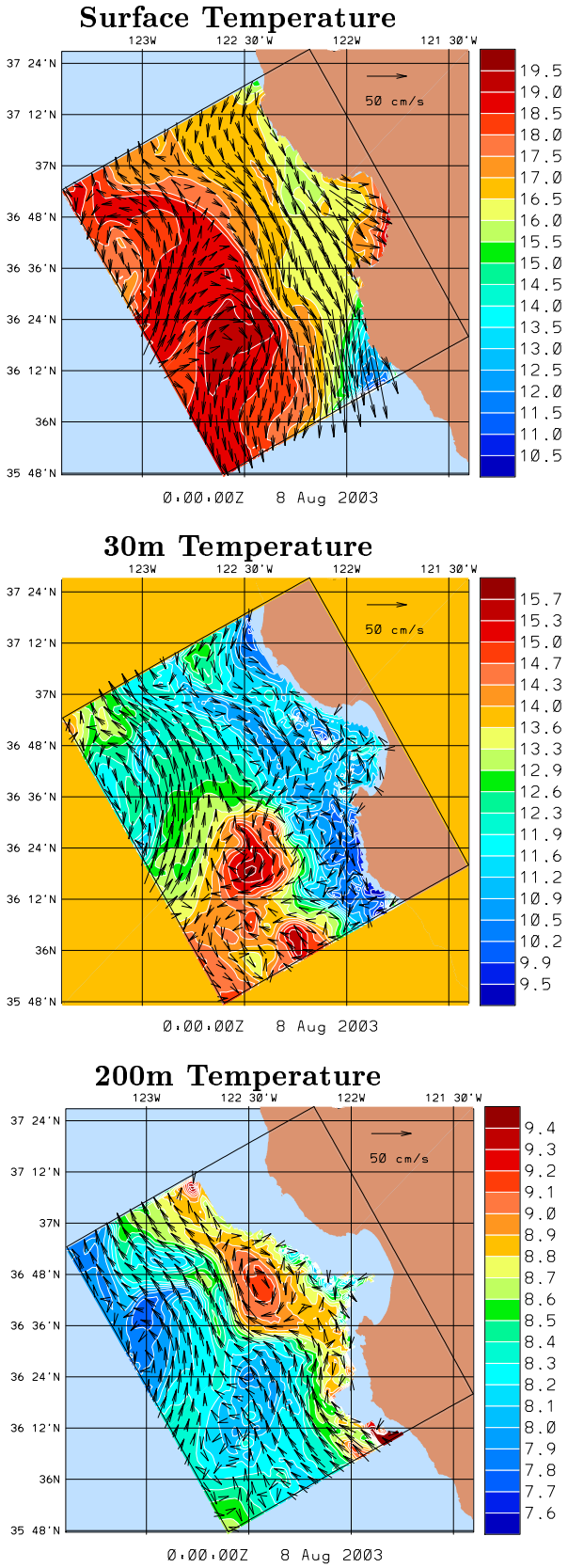

Figure 2: Typical temperature and velocity fields issued during real-time exercise.

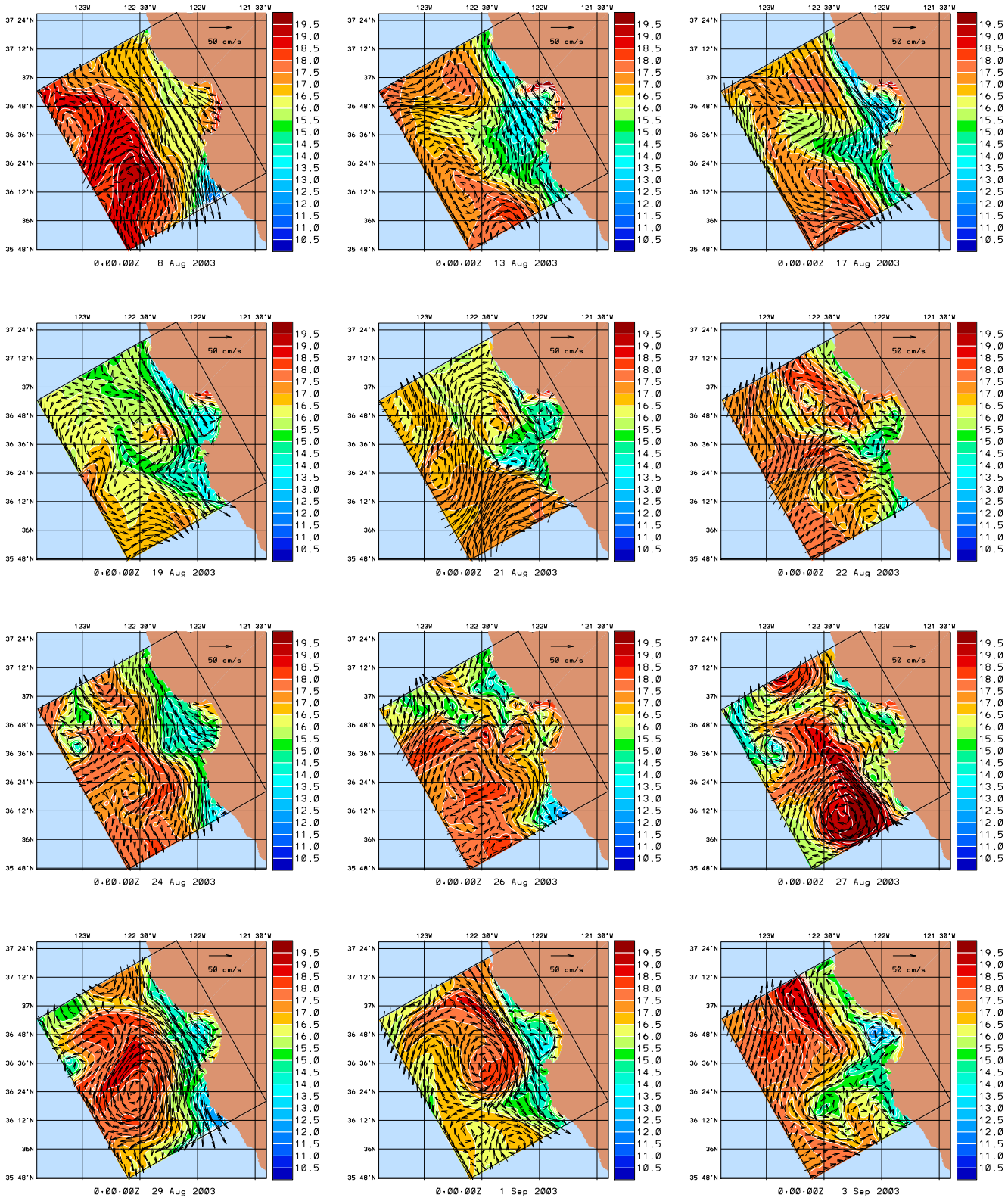

Figure 3: Surface temperature and velocity forecasts issued at various stages in the upwelling/relaxation cycle.

Stand Alone **Nested** **ESSE**

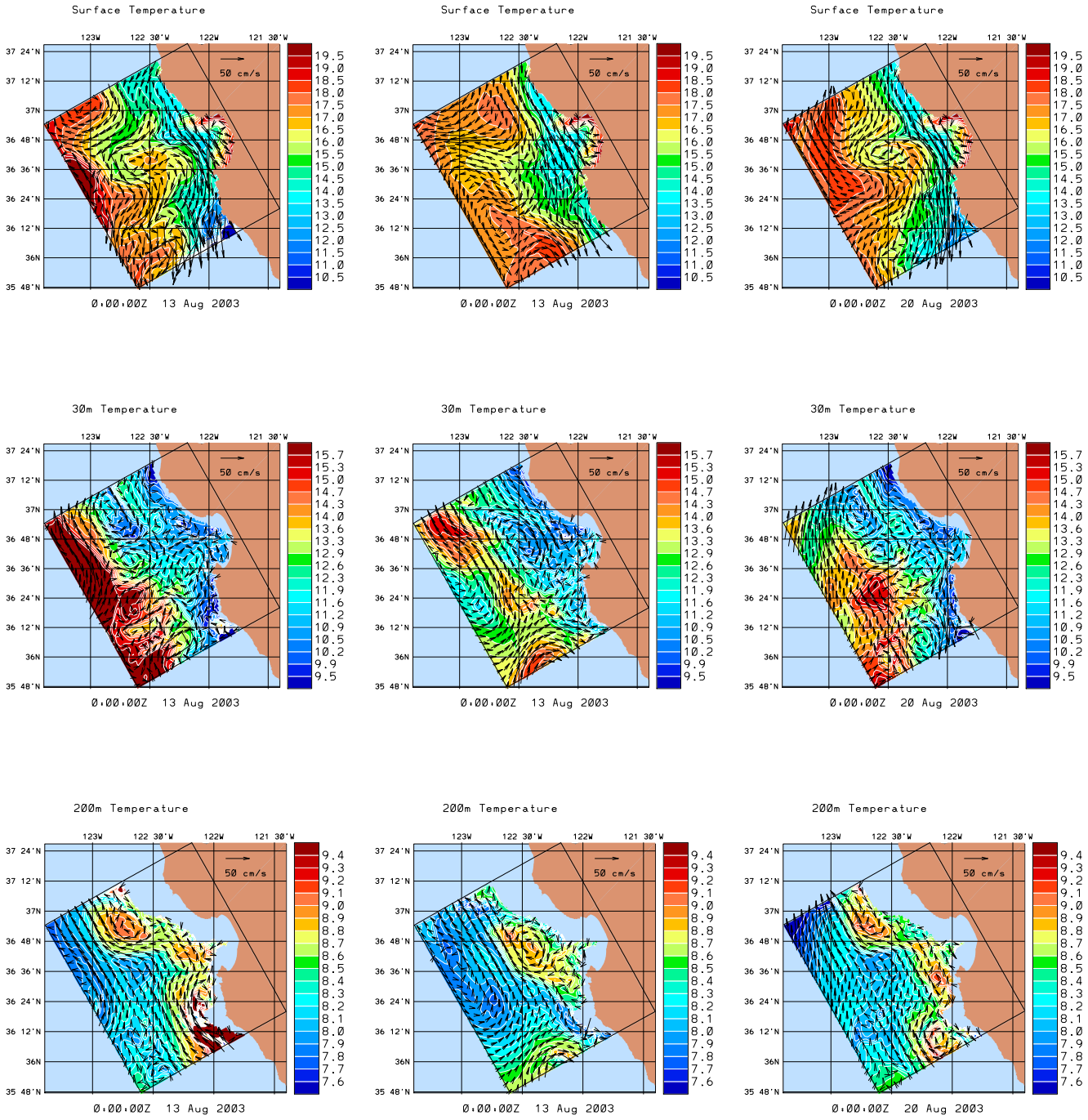

Figure 4: Comparison of stand-alone, nested and ESSE forecasts for 13 Aug 2003.

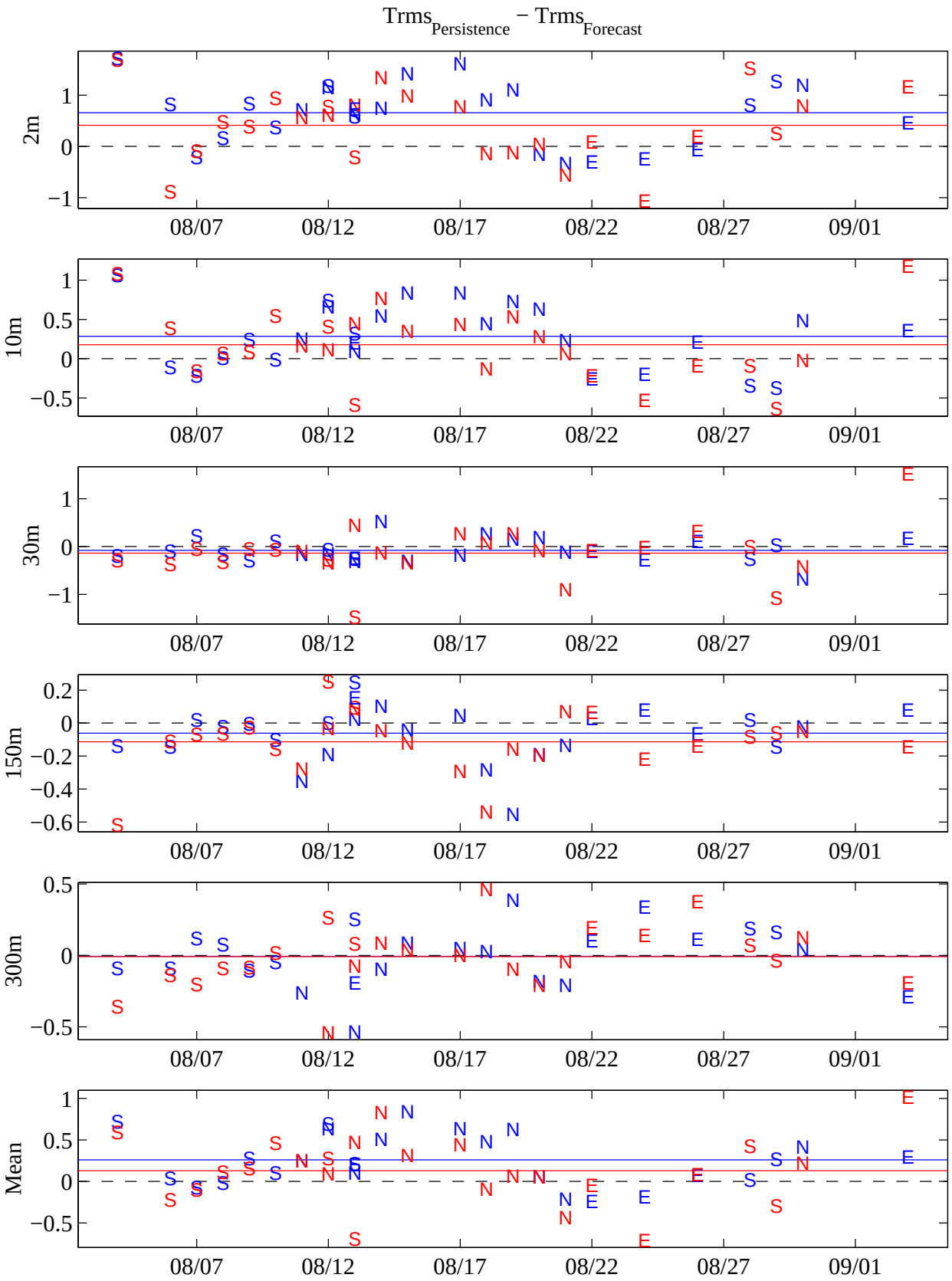

Figure 5: Real-time Temperature RMS errors.

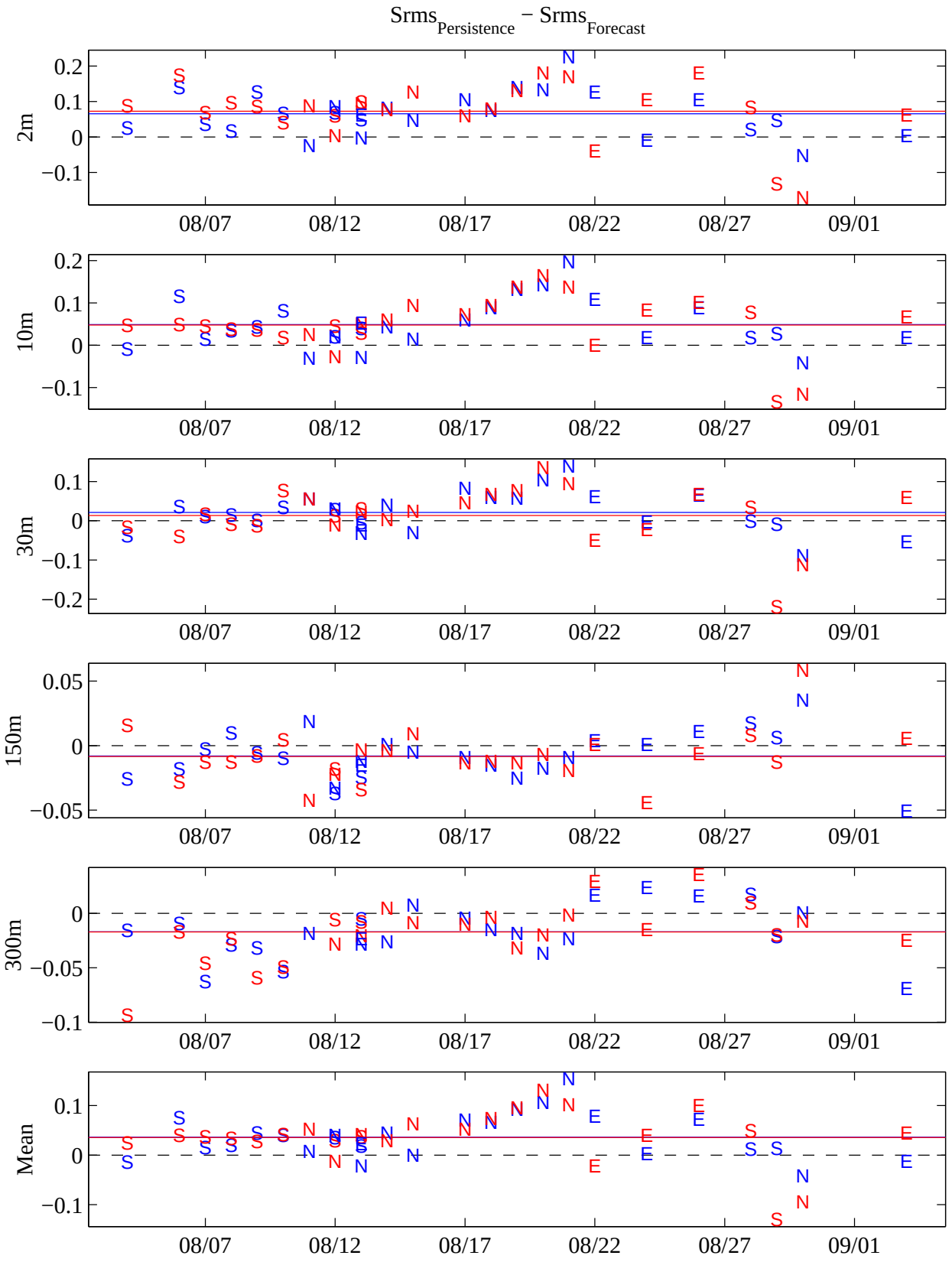

Figure 6: Real-time Salinity RMS errors.

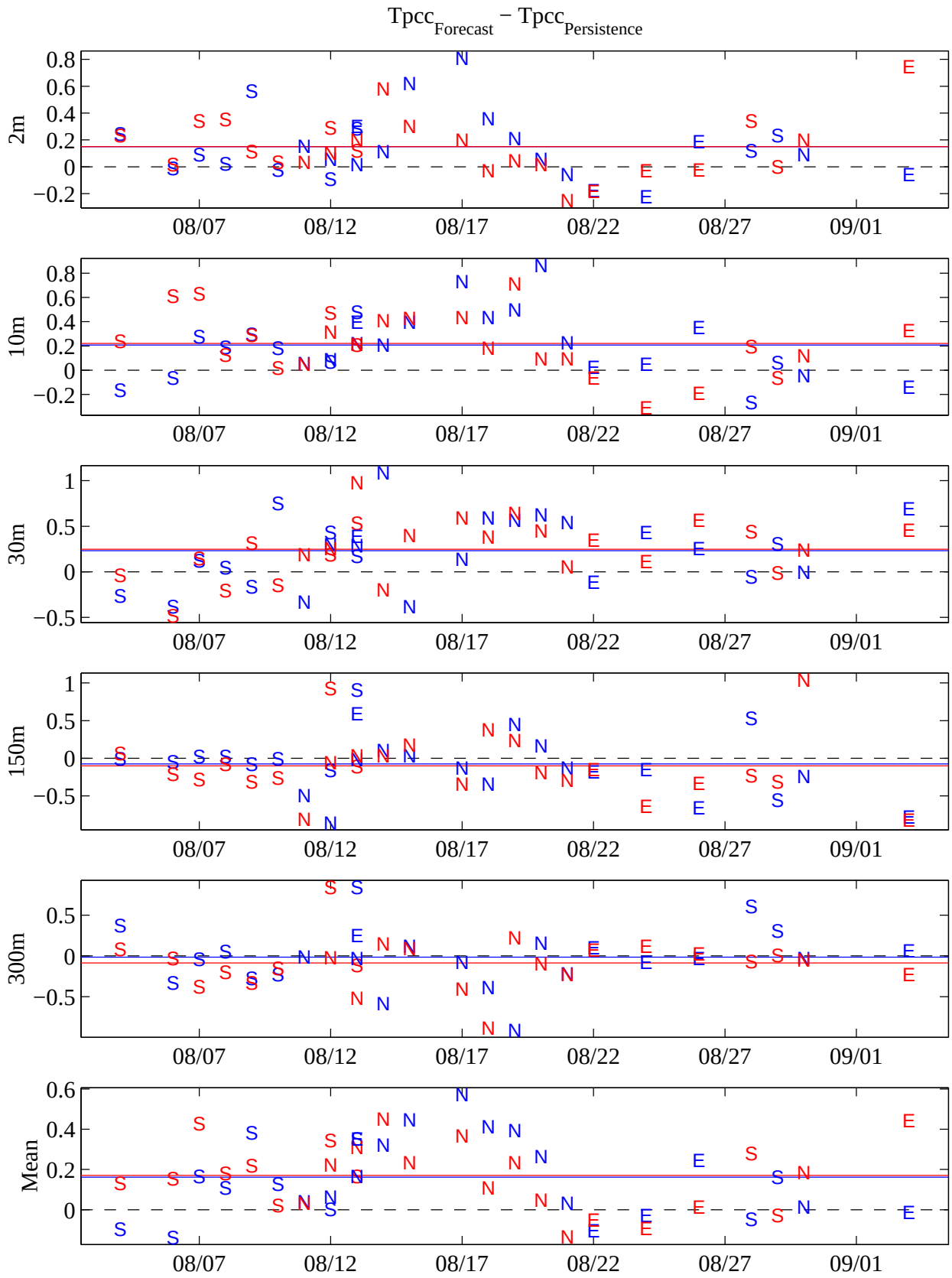

Figure 7: Real-time Temperature PCC.

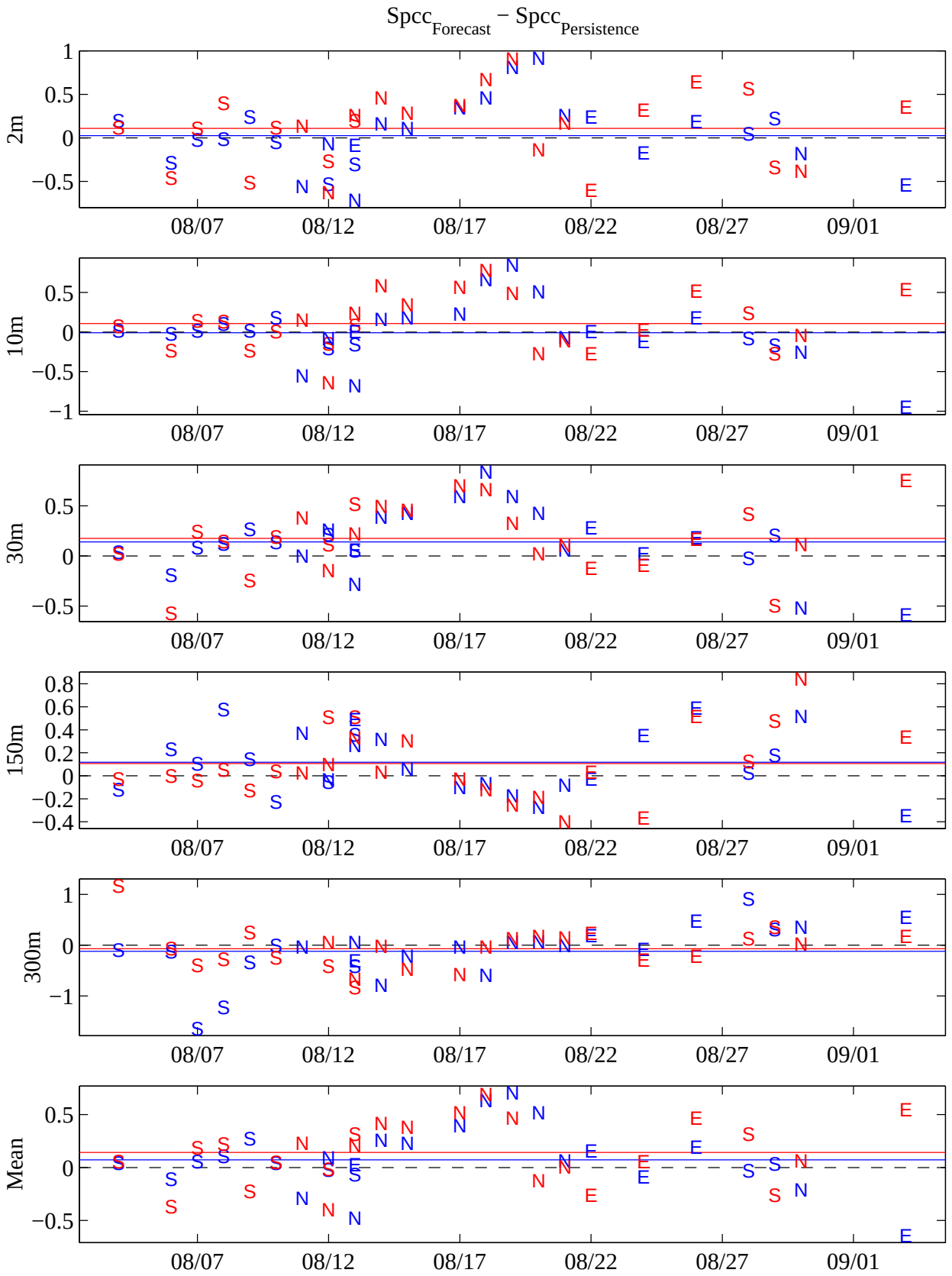

Figure 8: Real-time Salinity PCC.

References

Lermusiaux, P.F.J. (1997) Error Subspace Data Assimilation Methods for Ocean Field Estimation: Theory, Validation and Applications. *PhD Thesis*, Harvard University, Cambridge, MA.

Orlanski, I. (1976) A Simple Boundary Condition for Unbounded Hyperbolic Flows. *J. Comp. Phys.*, **21**. 251–269.

Pacanowski, R.C. and G.H. Philander (1981) Parameterization of Vertical Mixing in Numerical Models of Tropical Ocean. *J. Phys. Oceanogr.*, **11**, 1443–1451.

Perkins, A.L., L.F. Smedstad, D.W. Blake, G.W. Heburn, & A.J. Wallcraft (1997) A new nested boundary condition for a primitive equation ocean model. *J. Geophys. Res.*, **102**(C2). 3483–3500.

Spall, M.A. & A.R. Robinson (1989) A New Open Ocean, Hybrid Coordinate Primitive Equation Model. *Mathematics and Computers in Simulations*, **31**, 241–269.

Shapiro, R. (1970) Smoothing, Filtering and Boundary Effects. *Reviews of Geophysics and Space Physics*, **8**(2), 359–387.

Sloan, N.Q., III (1996) Dynamics of a Shelf-Slope Front: Process Studies and Data-Driven Simulations in the Middle Atlantic Bight. *PhD Thesis*, Harvard University, Cambridge, MA.